RSC Medicinal Chemistry

ROYAL SOCIETY OF CHEMISTRY

RESEARCH ARTICLE

View Article Online
View Journal | View Issue

Cite this: *RSC Med. Chem.*, 2024, **15**, 1556

A new class of 7-deazaguanine agents targeting autoimmune diseases: dramatic reduction of synovial fibroblast IL-6 production from human rheumatoid arthritis patients and improved performance against murine experimental autoimmune encephalomyelitis†

Michelle Cotter,[a] Shauna M. Quinn,[b] Ursula Fearon,[c] Sharon Ansboro,[c] Tatsiana Rakovic,[c] John M. Southern, *[a] Vincent P. Kelly *[b] and Stephen J. Connon *[a]

A simple *in vitro* assay involving the measurement of IL-6 production in human synovial fibroblasts from rheumatoid arthritis patients has been utilised to select candidates from a targeted library of queuine tRNA ribosyltransferase (QTRT) substrates for subsequent *in vivo* screening in murine experimental autoimmune encephalomyelitis (EAE – a model of multiple sclerosis). The *in vitro* activity assay discriminated between poor and excellent 7-deazaguanine QTRT substrates and allowed the identification of several structures which subsequently outperformed the previous lead in EAE. Two molecules were of significant promise: one rigidified analogue of the lead, and another considerably simpler structure incorporating an oxime motif which differs structurally from the lead to a considerable extent. These studies provide data from human cells for the first time and have expanded both the chemical space and current understanding of the structure–activity relationship underpinning the remarkable potential of 7-deazguanines in a Multiple Sclerosis disease model.

Received 12th January 2024,
Accepted 17th March 2024

DOI: 10.1039/d4md00028e

rsc.li/medchem

Introduction

Multiple sclerosis (MS) is the most common chronic autoimmune disease of the central nervous system[1] affecting *ca.* 3 million patients worldwide; with rising prevalance.[2] Considerable therapeutic strides have been made through the development of disease-modifying drugs – however a curative treatment remains elusive.[1,3] The search for new targets for the treatment of this multifaceted disease is hence both broadening and intensifying.[4]

Recently it has been shown that one such target is tRNA (**1**, Fig. 1). Queuine (**2**) is a hypermodified 7-deazaguanine nucleobase which is irreversibly incorporated (in place of an expelled existing guanine (**3**) base) into eukaryotic tRNAs **1** associated with histidine, tyrosine, aspartic acid and asparagine at the wobble position to give new queuosine-modified tRNA **4**.[5] This highly unusual reaction is catalysed by the heterodimeric enzyme queuine tRNA ribosyltransferase (QTRT, **5**).[6–10] Queuine is exclusively synthesised by

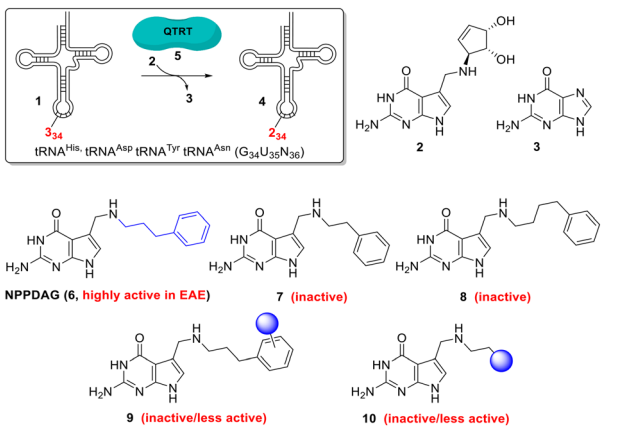

Fig. 1 The QTRT-catalysed wobble-base exchange reaction involving tRNA^{His,Asp,Tyr,Asn}, the structures of queuine, guanine, NPPDAG and related analogues.

[a] *School of Chemistry, Trinity College, Trinity Biomedical Sciences Institute, 152-160 Pearse Street, Dublin, Ireland. E-mail: southerj@tcd.ie, connons@tcd.ie*
[b] *School of Biochemistry & Immunology, Trinity College, Trinity Biomedical Sciences Institute, 152-160 Pearse Street, Dublin, Ireland. E-mail: kellyvp@tcd.ie*
[c] *School of Medicine, Trinity College, Trinity Biomedical Sciences Institute, 152-160 Pearse Street, Dublin, Ireland*

† Electronic supplementary information (ESI) available: Spectra for active compounds, figures related to PBMC cell viability and animal weights during treatment. See DOI: https://doi.org/10.1039/d4md00028e

eubacteria and must be obtained from either dietary sources or gut fauna by mammals,[11,12] it is not an essential nutrient in mice[13] however queuine-deprived mice exhibit a pathological sensitivity to tyrosine deficiency.[5] A comprehensive picture of queuine's biological *raison d'etre* has not emerged.

Modification of tRNA by queuine has been shown to play a role in the control of protein translational speed/folding and codon usage bias.[14,15] Influence over cell proliferation[5] and metabolism[16] has been demonstrated; levels of queuine modification have been correlated with age/cellular differentiation stage[17–19] and negatively correlated with the progression of several cancers.[20–22] These modalities of influence associated with queuine are interesting in the context of the growing attention being directed at potential treatments for MS based on promoting differentiation to regulatory T- (T_{reg}) cells.[4,23,24]

While QTRT will catalyse the base exchange exclusively involving the 4 aforementioned tRNAs and eschew the modification of the myriad of other RNA molecules in the cell,[25] it exhibits a surprisingly wide substrate scope with respect to the deazaguanine component.[25,26] This allows the possibility of exploiting QTRT to rapidly, conveniently and dramatically alter the properties of tRNA at the anticodon loop, provided that it has not already been elaborated with queuine. Hypomodification by queuine is a characteristic of undifferentiated, rapidly proliferating cells[20–22,27,28] and thus by extension we hypothesised that tRNA in clonally expanding T-cells could be susceptible to modification with artificial nucleobases in a fashion that mature, terminally differentiated cells would not. This would allow the selective targeting of a subset of the proliferative T-cells driving autoimmune disease in a way to which the majority of cell populations are inert. We previously reported the synthesis and evaluation of the deazaguanine NPPDAG (**6**, Fig. 1) in murine experimental autoimmune encephalomyelitis (EAE).[28] The artificial nucleobase is a substrate for QTRT and is incorporated into tRNA while avoiding genotoxicity through the action of the hypoxanthine–guanine phosphoribosyltransferase (HPRT) enzyme. NPPDAG possessed unprecedented activity: administration of 5 daily doses (30 mg Kg^{-1}) led to complete symptom remission, while QTRT-deficient mice were refractory to therapy. Levels of effector and cytotoxic T-cells in both the periphery and the brain of treated animals were markedly reduced without overt immunosuppression *via* general lymphocyte population diminution. Spleen cells from NPPDAG-treated animals remained functional – they proliferated normally in the presence of a pan-stimulant yet remained unresponsive when re-exposed to EAE-inducing antigen.

NPPDAG represents a queuine analogue where the aminomethyl-7-deazaguanine moiety has been retained and the cyclopentene diol unit has been exchanged for a substituent comprising a 3-carbon chain and an aromatic ring (highlighted in blue in structure **6**). Subsequent studies[29] aimed at optimising the structure of this substituent revealed an exceptionally narrow structure–activity relationship in the context of EAE treatment (*i.e.* through the modification of the behaviour of tRNA by the covalently incorporated artificial nucleobase). For instance, despite demonstrably serving as efficient QTRT substrates; both 2- and 4-carbon chain analogues (**7** and **8** respectively, Fig. 1) were inactive as immunomodulatory agents, as were the vast majority of variants incorporating substituted benzene rings of general type **9** (electron withdrawing/electron donating substituents, ring extensions, heterocyclic analogues (save a 3-thiophenyl isostere), protic substituents, all substitution patterns). Removal of the aromatic ring and replacement with either aliphatic chains or queuine-fragments (*i.e.* **10**, Fig. 1) were also not advantageous.

Results and discussion

Compound efficacy was initially determined using two *in vitro* assays – a screen monitoring the secretion of IFN-γ by spleen cells from EAE-diseased mice and a $CD3^+$ T cell proliferation assay involving spleen cells. Both assays used cells from wildtype and QTRT-deficient mice. If sufficiently active, screening progressed to the murine EAE model.[29] While this regime allowed the identification of potentially efficacious candidate molecules, we wished to develop a more streamlined initial screening methodology – preferably not reliant on a two-assay system and the availability of cells from EAE-diseased animals.

In addition, we were interested in the activity of NPPDAG and variants as potential treatments of rheumatoid arthritis (RA) – a painful and mobility-attenuating chronic condition among the most prevalent autoimmune diseases which affects *ca.* 1% of the global population.[30] While RA and MS are distinct and complex multi-faceted autoimmune conditions, the contributions from activated macrophages, Th1 and Th17 cells (which are key in MS) towards driving RA are significant,[31] and we had shown that deazaguanine analogues could significantly reduce the populations of these (*inter alia*) pathological cells in EAE diseased mice.[28] Given that the mode of action of NPPDAG is not confined exclusively to direct effects on T-cells, we arrived at an unusual hypothesis: that evaluation of the influence of NPPDAG analogues on synovial fibroblasts from human RA patients (based on changes in concentrations of the signature cytokine IL-6 (ref. 32)) could not only serve as a simple screen to establish if deazaguanines could be active in RA, it could also possess predictive utility in EAE and additionally provide useful information regarding the behavior of these compounds in human cells. In this regard we note that dimethyl fumarate – an FDA-approved drug for use in MS and psoriasis which influences the proinflammatory Th17–Th1 response – has very recently shown promise in reducing IL-6 levels from fibroblast-like synoviocytes from human RA patients.[33,34]

In preliminary experiments, synovial fibroblasts from RA patients were activated with TNF-α and treated with NPPDAG (**6**) at either 100 μM or 200 μM and the levels of the pro-inflammatory cytokine IL-6 measured using an ELISA assay.

DMSO (4% in PBS buffer) was utilised as a control. Gratifyingly, a dose-dependent reduction in the cytokine concentration was observed after 72 h (Fig. 2).

With proof of concept in human RA synovial fibroblasts in hand, attention now switched to the activity of NPPDAG analogues. Earlier studies[29] had shown that changes to the length of the linker chain associated with NPPDAG led to compounds inactive in EAE screening this constraint, coupled with the requirement for a simple aromatic moiety at the chain terminus, pointed to a requirement for the NPPDAG side chain to attain a particular conformation to alter the properties of the tRNA anticodon loop. We therefore began with retention of the NPPDAG structural core and a focus on mild rigidification of the linker chain *via* substitution (Fig. 3). All compounds were evaluated at 200 μM concentrations and unless stated, were excellent substrates for QTRT and could be incorporated into tRNA.[25] DMSO (4% in PBS buffer) was again used as a control, alongside IgG and positive controls (Tofacitinib – Pfizer, Janus kinase inhibitor, 1 μM) and Adalimumab (Humira – Abbvie, anti-TNF-α monoclonal antibody, 1 μM).

The 3-thiophene derivative **11** was previously[29] shown to possess potent *in vitro* activity in cells from EAE-diseased mice but was not evaluated in EAE itself – here it proved capable of lowering IL-6 production relative to vehicle control, with activity levels close to those obtained using **6**. Methyl substitution at the benzylic position (*i.e.* racemate **12**) resulted in modest improvement, while the (*R*)-enantiomer of the same compound (*i.e.* **13**) was essentially inactive. This would signal significant activity associated with the (*S*)-antipode, which was not synthesised due to improved activity obtained from simpler materials in the study. Installation of a second phenyl unit at the same position gave rise to **14**, which possessed activity levels akin to **11**; while hydroxyl substitution at the benzylic position (*i.e.* enantiomers **15** and **16**) seemed only marginally advantageous where the stereogenic center had the (*S*)-configuration.

With little achieved from mono-substitution at the benzylic position, *gem*-disubstituted analogues were next evaluated. These, it was envisaged, would be significantly less conformationally flexible than NPPDAG itself, without being considered rigid materials. The dimethyl derivative **17** exhibited markedly improved activity – considerably superior to either NPPDAG or any of the mono-substituted derivatives **11–16**. Augmentation of the steric demand at the quaternary carbon atom (*i.e.* **18**) resulted in a less dramatic fall in IL-6 concentration, however it should be noted that the substrate

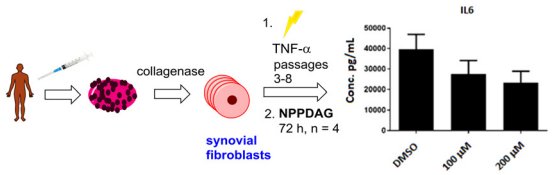

Fig. 2 Reduction in production of IL-6 by synovial fibroblasts from RA patients in the presence of **NPPDAG**.

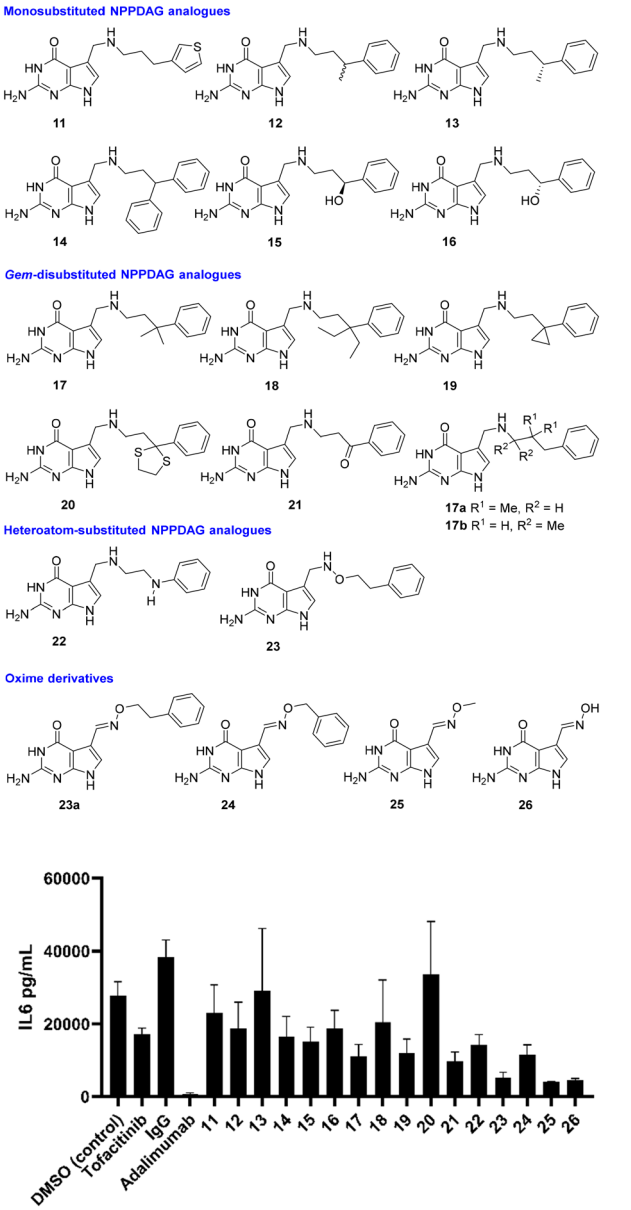

Fig. 3 Reduction in production of IL-6 by synovial fibroblasts from RA patients in the presence of a library of **NPPDAG** derivatives.

competency of **18** toward QTRT is <20% of that associated with **6**.[25] The smaller *gem*-disubstituted cyclopropyl analogue **19** also exhibited impressive activity – albeit to a lesser extent than observed using **17**.

Consistent with this trend was the poor performance of the dithiolane **20** (bulky benzylic position, mediocre QTRT compatibility) and the excellent activity detected in experiments involving the less sterically demanding precursor ketone **21** – which could be readily manipulated by QTRT.[25] While it is tempting to consider the electronic effect of the ketone on the aromatic ring, we have previously shown (multiple examples) that the installation of electron withdrawing substituents either on or in the ring was not advantageous[29] – thus, at this juncture we would suggest that activity here could be primarily

due to rigidification. Given the superiority of **17** over **6** (Fig. 1 and 3), isomers **17a–b** were synthesised where the *gem*-dimethyl unit was relocated to either the middle of the chain or adjacent to the secondary amine group. The former material was highly insoluble and the latter a poor QTRT substrate,[25] so neither were carried forward for screening.

The final module of screening in RA was intended to be a short examination of the influence of heteroatoms in the chain itself, as exemplified by the aniline derivative **22** and the alkoxyamine **23**. Interestingly, both proved capable of ameliorating the production of IL-6 to a greater degree than **6**, with **23** proving the most potent compound screened thus far. The factors underpinning the striking increase in potency associated with **23** were not immediately obvious. With an initial view to investigating the effects of further rigidification on *in vitro* compound behaviour, we prepared **23a** – the (*E*)-oxime variant of **23**. This compound was a completely incompetent substrate for QTRT[25] and was not subsequently evaluated in the synovial fibroblast assay. The homologue with a chain shorter by one methylene unit however (*i.e.* **24**) proved approximately as active as **17** – which is extraordinary in light of the fact that it does not possess a chain of sufficient length between the exocyclic *N*-atom and the aromatic ring to be compatible with the established SAR (see Fig. 1).[29] Accordingly, simple *O*-methyl-substituted and unsubstituted oxime derivatives of 7-deazaguanine (*i.e.* **25** and **26**) were evaluated. These are excellent QTRT substrates[25] which led to the lowest IL-6 concentrations detected in the study.

The synovial fibroblast screen identified a number of analogues of **6** which served as excellent QTRT substrates and possessed significantly superior activity to the lead structure (*e.g.* **17**, **21** and **23**). In addition, 2 simple oximes with structures not anticipated to be consistent with activity showed particular promise. Returning to our initial hypothesis regarding the predictive power of the synovial fibroblast assay in identifying candidates for screening in EAE, a selection of these compounds were evaluated *in vivo* in chronic, monophasic, myelin oligodendrocyte glycoprotein (MOG_{33-35})-mediated murine EAE (Fig. 4). Mice were treated daily *via* intraperitoneal injection when a disease score 2 (limp tail, wobbly gait – usually 9 days post immunisation) was attained. A lower dose equimolar to 15 mg Kg^{-1} of NPPDAG (30 mg Kg^{-1} of NPPDAG leads to full remission) was utilised to facilitate efficacy comparisons.

On treatment with **6**, the disease course diverged from the controls after one day: progression peaked at day 3 post treatment and the animals condition gradually improved thereafter to a final disease score just under 3 after 7 days – consistent with earlier studies using **6** at this lower dose.[28] Gratifyingly, administration of compound **17** – the *gem*-dimethyl analogue of **6** – resulted in a peak at day 2, a more rapid disease remission and an improved final score. The ketone **21** also proved capable of arresting disease progression after one day of treatment, but does not appear as efficacious overall as **17**. The more difficult-to-synthesise **23** was not selected for full evaluation, however in a 4 day

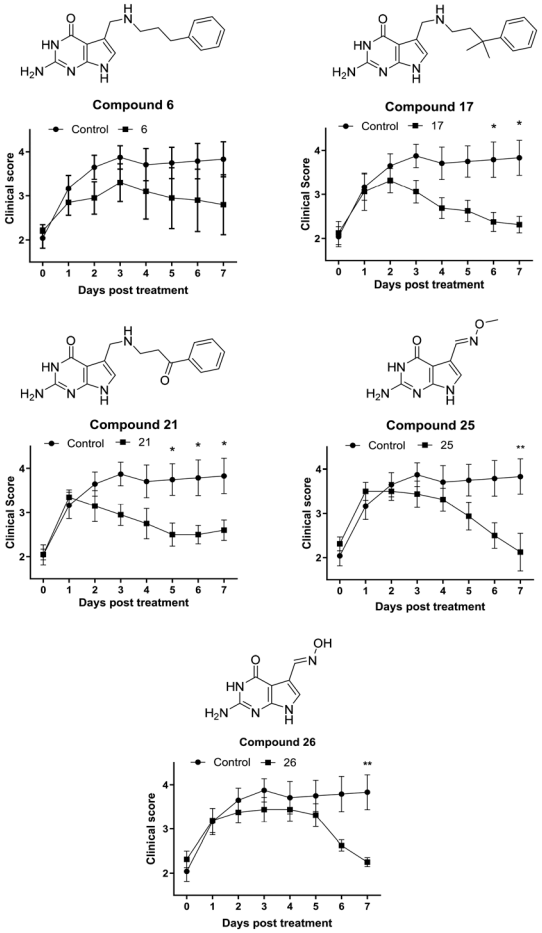

Fig. 4 Evaluation of selected compounds in EAE. Upon reaching a clinical score of approximately 2, EAE diseased female mice were administered PBS as control or equimolar concentrations of **6** (15 mg Kg^{-1}), **17** (16 mg Kg^{-1}), **21** (16 mg Kg^{-1}) **25** (9 mg Kg^{-1}) or **26** (9 mg kg^{-1}) *i.p.* daily for 7 days, n = 5. Animals were monitored daily for clinical score. Data represent the mean ± S.E.M. $^{*}P < 0.05$, $^{**}P < 0.01$, by two-way Anova with *post hoc* pair-wise comparison.

treatment study it performed similarly to **17** (data not shown). The methyl-oxime **25** exhibited a small deviation in behavior – again disease progression was arrested after one day of treatment, followed by 3 days of modest improvement. Thereafter remission was more rapid – with the animals returning to a disease score of 2 after 7 days. Its *O*-unsubstituted analogue **26** displayed a similar profile – albeit with a longer plateau phase post treatment and a marginally higher final disease score.

Experimental

In vitro rheumatoid arthritis synovial fibroblast (RASFC) assays

Patient recruitment and arthroscopy. Rheumatoid arthritis (RA) patients were recruited from the Rheumatology Department, St. Vincent's University Hospital. Patients gave fully informed written consent approved by the St Vincent's University Hospital Research Ethics Committee and research was performed in accordance with the Declaration of Helsinki.

Synovial tissue biopsies were obtained at arthroscopy under local anaesthetic using a Wolf 2.7 mm telescope (Wolf – Germany). Biopsies were used for isolation of primary RA synovial fibroblasts (RASFC). Paired peripheral blood mononuclear cells (PBMCs) were also isolated from RA patients.

Isolation of primary fibroblasts. RA synovial biopsies were digested with 1 mg mL^{-1} collagenase type 1 (Worthington Biochemical, Freehold, NJ, USA) in RPMI-1640 (Gibco-BRL, Paisley, UK) for 4 h at 37 °C in humidified air with 5% CO_2. Dissociated cells were grown to confluence in RPMI 1640, 10% FCS (Gibco-BRL), 10 mL of 1 mmol l^{-1} HEPES (Gibco-BRL), penicillin (100 units per mL; Bioscience), streptomycin (100 units per mL; Bioscience) and fungizone (0.25 μg mL^{-1}; Bioscience) before passaging. Cells were used between passages 3–8.

Compound screening. Initial screening compound **6** – RA synovial fibroblasts (RASFCs) from four individual patients were grown to 80% confluency in 48 well plates and treated with TNFα (10 ng mL^{-1}) in the presence of either 100 μM or 200 μM compound **6**. Media was replaced after 24 h and both fresh media and compound added. Cell supernatants were harvested at the 72 h time point and cytokine secretion analysed by ELISA. This was compared to DMSO control.

Screening compounds 11–26. RASFC cultures from different patients (n = 6 compounds **11**, **12**, **13**, **14**, **15**, **16**, **17**, **18**, **19**, **20**, **22**, **23**; n = 3 compounds **21**, **24**, **25**, **26**) were treated with TNFα (10 ng mL^{-1}) in the presence of controls or queuine analogues at a concentration of 200 μm. Culture media was replaced after 24 h and fresh media and compound were added. Cell supernatants were collected at the 72 h time point and tested for IL-6 secretion by ELISA. DMSO (4% in PBS), Tofacitinib (Xeljanz – Pfizer, Janus kinase inhibitor, 1 μM), IgG isotype antibody (1 μM) and Adalimumab (Humira – Abbvie, anti-TNF monoclonal antibody, 1 μM) served as experimental controls.

Cytokine analysis. The pro-inflammatory cytokine IL-6 was quantified in RASFCs cultured supernatants by ELISA (R&D systems, UK) according to manufacturer's instructions.

PBMC toxicity screen

To ensure that the reductions seen in IL-6 were not the result of compound toxicity, tests were performed on matched PBMCs. PBMCs were isolated from whole blood by Ficoll density gradient centrifugation (Lymphoprep™; STEMCELL technologies, Canada) and were incubated for 24 h with the selected compounds at four different concentrations (5, 50, 100 and 200 μM) as well as DMSO controls as shown. Cells were then washed in PBS and stained with a Near IR viability dye for 30 min. Cells were washed and immediately analysed on a flow cytometer. PBMC cell viability assays for selected compounds can be found in the ESI† (Fig. S1).

In vivo experimental autoimmune encephalomyelitis (EAE) experiments[35]

For EAE studies, mice were maintained under specific pathogen-free conditions. Experiments were conducted under licence from the Health Products Regulatory Authority (Ref: A19136/P086), with the approval of the Trinity College Dublin Animal Research Ethics Committee.

Preparation of reagents for the EAE study.

- **C57BL/6 female mice** were delivered 6–8 weeks old (Harlan labs), and disease induced in animals of approximately 20 g weight and around 10–12 weeks old at time of disease initiation.
- **Complete Freund's Adjuvant (CFA)** was prepared by diluting complete Freund's adjuvant (4 mg mL^{-1} *M. tuberculosis*; Chondrex) to a concentration of 2 mg mL^{-1} in incomplete Freund's adjuvant.
- **MOG solution** was prepared by re-suspending an appropriate amount of mouse $MOG_{(35-55)}$ peptide (GenScript; supplied frozen down as a powder) in PBS (Sigma) to give a stock solution of 5 mg mL^{-1}.
- **CFA/MOG Emulsion** comprised a 50% suspension of CFA, 10% MOG solution in 40% PBS solution (*i.e.* 10% of the solution above). It was prepared by the following method:

a. PBS solution and MOG solution were first placed into a 50 ml plastic tube with CFA subsequently placed on top.

b. The mixture was homogenised using a laboratory bench homogeniser at a speed of 13 500 rpm, until the tube can be turned upside down without the emulsion spilling. The correct consistency of the MOG emulsion is necessary to ensure dispersion does not occur in the animal after administration. The consistency was tested as follows: PBS solution was placed in a petri dish. MOG emulsion was withdrawn from the 50 mL tube with a syringe using a blue pipette tip. A drop of MOG emulsion was added to the PBS. A correct preparation should maintain its consistency and not disperse into the PBS.

c. Once prepared, the emulsion was loaded into a 1 mL Tuberculin syringe fitted with a 23 Gauge needle.

- **Pertussis toxin (PT; Katetsuken)** was made up in the morning of disease induction, with sufficient volume prepared for both day 0 and day 2 injections. PT stock was 200 μg ml^{-1} which equals 200 ng μL^{-1}. Each mouse was injected with 200 ng (equating to 1 μL of PT stock) in 200 μL PBS.

Induction of disease.

- Day 0

a. The mice were weighed and marked with a permanent marker on the tail.

b. Each mouse was injected intraperitoneally with 200 μL of PT (tuberculin syringe and a 27 Gauge needle).

c. Subsequently, each mouse was subcutaneously injected on the back with 200 μL of CFA/MOG.

- Day 2

a. Each mouse was weighed again.

b. Animals were injected intraperitoneally with 200 μL of PT prepared previously.

- Day 5-onwards

a. The mice were weighed every day and the data recorded.

b. The first day of overt disease occurs approximately from day 9 onwards.

Clinical scoring of the diseased animals. The first indication of disease in this model is characterised by loss of body weight with a clinical score of 1 assigned to 1 g body

weight loss and loss of power in the tail. Note: mice are checked at the same time each day as weights can vary between morning and evening, diseased mice were scored as follows:

0.25 little or no weight loss, but loss of power in the tip of the tail.

0.5 small amount of weight loss, but loss of power to half of the tail.

1.0 small amount of weight loss, but loss of power to entire tail.

1.25/1.5 increased body weight loss and some loss in tail power.

2.0 characteristic cowboy gait (animal rear extended).

2.5 characteristic cowboy gait with maintained ability to support rear.

3.0 movement of rear legs, but unable to support rear.

3.5 loss of movement in only one rear leg and unable to support rear.

3.75 loss of rear leg movement and unable to support rear.

4.0 complete loss of movement in rear legs with locomotion using only front legs.

4.25/4.5 weak front leg movement and complete paralysis of rear.

4.5 animal locomotion considered severe enough to euthanise the animal.

5.0 any animal discovered dead overnight.

Compound preparation. Compounds in powder format were made up fresh each day in DMSO (Sigma) and diluted to a concentration of 4 mM in 4% DMSO/PBS using PBS as follows:

- A 100 mM solution of dry, powdered compound was prepared in DMSO.

- The 100 mM stock was diluted 25 fold in PBS to give a compound concentration of 4 mM.

- Each mouse was injected intraperitoneally with 200 μL of diluted compound everyday for 7 days.

- This approach allowed the assessment of compounds on an equimolar basis to alleviate effects influenced by the different molecular weight of the compounds.

Compound administration. EAE diseased animals were inducted onto the study when they had reached a disease score of between 1.5 and 2. The animals were marked on the tails and randomly assigned to treatment and control groups and treated daily (at equimolar levels) for 7 days (unless otherwise stated) as follows:

- Control animals administered PBS solution containing 4% DMSO (n = 6).

- Compound **6** treated animals, 15 mg Kg^{-1} (n = 5).

- Compound **7** treated animals, 16 mg Kg^{-1} (n = 4).

- Compound **21** treated animals, 16 mg Kg^{-1} (n = 5).

- Compound **23** treated animals, 15 mg Kg^{-1} (n = 5, 4 day study).

- Compound **25** treated animals, 9 mg Kg^{-1} (n = 4).

- Compound **26** treated animals, 9 mg Kg^{-1} (n = 4).

Animals that failed to succumb to disease or whose disease had progressed to a score of 3 or beyond were not included in the study.

Graphing results. The clinical scores for the mice were graphed by days post treatment. Day 0 was when the mouse reaches a clinical score of approximately 2 (identified upon inspection of the animals each morning). At this point the animal receives its first injection of control or queuine analogue. Each mouse was tracked individually, scored and weighed until the day after the last injection. Data was plotted using Prism Software (GraphPad, USA) and analysed using two-way ANOVA (*i.e.* variables of time and treatment) with multiple comparisons.

Analysis of animal weights. In order to provide observer-independent tracking of disease severity weights of the animals were recorded on a daily basis at the same time clinical score was assessed. The changes in weight associated with treatment involving selected compounds can be seen in the ESI† (Fig. S2).

Deazaguanine substrates

Compounds **6**, **11**–**26** were prepared previously to evaluate their QTRT compatibility and their characterisation – melting points, HRMS and copies of the associated ^{1}H NMR and ^{13}C NMR spectra which attest to >95% purity have been reported.[25,28,29] The synthesis of key compounds **6**, **17**, **21**, **25** and **26** evaluated in EAE are described below – associated ^{1}H- and ^{13}C NMR spectra have been provided in the ESI.†

General

Proton nuclear magnetic resonance spectra were recorded on a Bruker 400 MHz or 600 MHz (as specified) or Agilent 400 MHz spectrometer in DMSO-d_6 relative to residual DMSO (δ = 2.50 ppm). Chemical shifts are reported in ppm and coupling constants in Hertz. Carbon (100 MHz and 150 MHz) spectra were recorded on the same instruments with total proton decoupling. All melting points are uncorrected. Infrared spectra were obtained on a Perkin Elmer spectrophotometer. Flash chromatography was carried out using silica gel, particle size 0.04–0.063 mm. TLC analysis was performed on precoated $60F_{254}$ slides, and visualised by either UV irradiation, $KMnO_4$ staining, or phosphomolybdic acid staining as appropriate. All chemicals were obtained from commercial sources and used as received unless otherwise stated.

General procedure A: synthesis amine hydrochloride salts

2-Amino-5-(((3-phenylpropyl)amino)methyl)-3,7-dihydro-4*H*-pyrrolo[2,3-*d*]pyrimidin-4-one·HCl (6). To a suspension of *N*-((4-oxo-2-(tritylamino)-4,7-dihydro-3*H*-pyrrolo[2,3-d]-pyrimidin-5-yl)methyl)formamide (200 mg, 0.48 mmol) and Na_2SO_4 (5 mg) in MeOH (5 mL) was added the appropriate amine, in this case 3-phenylpropylamine (74 μL, 0.52 mmol) and the resulting suspension stirred at room temperature until complete consumption of aldehyde starting material was observed by TLC analysis. Solid sodium borohydride (1.43 mmol, 55.00 mg) was added and the reaction mixture stirred at room temperature for a further hour. Water (5 mL) was added and the resulting suspension stirred for 10 min

before being extracted with dichloromethane (3 × 5 mL). The combined organic layers were dried ($MgSO_4$) and concentrated *in vacuo* to yield the crude product which was purified by flash chromatography (9 : 1 dichloromethane : methanol) to yield the desired compound as a white solid (210 mg, 81%), m.p. > 300 °C (decomp.).

A solution of the trityl-protected compound (210.0 mg, 0.39 mmol) in 1.25 M methanolic HCl (3 mL) was prepared and stirred at room temperature for 16 h. The precipitated product was removed by filtration and washed with dichloromethane to yield the title compound as a white powder, (84 mg, 65%, 53% over two steps), m.p. >300 °C (decomp.). ^{1}H NMR (400 MHz, DMSO-d_6) δ 1.84–1.98 (2H, m), 2.63 (2H, t, J 7.6), 2.85–2.95 (2H, m), 4.13 (2H, t, J 4.8), 6.51 (2H, bs, NH), 6.80 (1H, s), 7.14–7.21 (3H, m), 7.23–7.30 (2H, m), 9.10 (2H, bs, NH), 11.02 (1H, bs, NH), 11.29 (1H, bs, NH). ^{13}C NMR (150 MHz, DMSO-d_6): δ 27.7, 32.3, 43.0, 45.6, 98.7, 108.9, 117.9, 126.5, 128.7, 128.9, 141.1, 152.6, 153.4, 160.7. HRMS (m/z ESI$^+$): found: 298.1662 ([M + H]$^+$; $C_{16}H_{20}N_5O$ requires: 298.1668). ν_{max} (film)/cm^{-1}: 1456, 1625, 2443, 2713, 2756, 2873, 2933, 3184.

2-Amino-5-(((3-methyl-3-phenylbutyl)amino)methyl)-3,7-dihydro-4*H*-pyrrolo[2,3-*d*]pyrimidin-4-one·HCl (17). Prepared as per general procedure **A**, however, the title compound is soluble in methanol and, thus, does not precipitate to a large extent so diethyl ether was added to induce selective precipitation of the final product. The product was filtered and washed with Et_2O to yield the title compound as a white powder (18 mg, 51%), m.p. >300 °C. ^{1}H NMR (400 MHz, DMSO-d_6): δ 1.23 (6H, s), 1.92–1.99 (2H, m), 2.58–2.63 (2H, m), 4.05 (2H, t, J 4.0), 6.65 (2H, bs), 6.71 (1H, d, J 1.9), 7.10–7.16 (1H, m), 7.23–7.32 (4H, m), 9.06 (2H, bs), 11.15 (1H, bs), 11.32 (1H, bs). ^{13}C NMR (100 MHz, DMSO-d_6): δ 29.1, 36.9, 39.1, 42.1, 42.8, 98.8, 109.2, 118.7, 125.9, 126.3, 128.7, 146.9, 147.7, 152.6, 159.4. HRMS (m/z – ESI): found: 326.1975 ([M + H]$^+$ $C_{18}H_{24}N_5O$; requires: 326.1981). ν_{max} (film)/cm^{-1}: 1066, 1551, 1654, 2901, 2987, 3685.

2-Amino-5-(((3-oxo-3-phenylpropyl)amino)methyl)-3,7-dihydro-4*H*-pyrrolo[2,3-*d*]pyrimidin-4-one·HCl (21). Prepared as per general procedure **A** to yield the title compound as a white powder (53 mg, 32%), m.p.: >250 °C (decomp.). ^{1}H NMR (400 MHz, DMSO-d_6): δ 3.23–3.31 (2H, m), 3.45–3.52 (2H, m), 4.20 (2H, t, J 5.1), 6.40 (2H, bs), 6.82 (1H, d, J 2.1), 7.53 (2H, t, J 8.0), 7.62–7.68 (1H, m), 7.90–7.96 (2H, m), 9.00 (2H, bs), 10.90 (1H, bs), 11.27 (1H, bs). ^{13}C NMR (100 MHz, DMSO-d_6): δ 34.9, 41.3, 42.8, 99.0, 109.1, 118.8, 128.4, 129.3, 134.1, 136.3, 147.6, 152.8, 159.6, 197.4. HRMS (m/z – APCI): found: 312.1453 ([M + H]$^+$ $C_{16}H_{18}N_5O_2$; requires: 312.1460). ν_{max} (film)/cm^{-1}: 1579, 1623, 1671, 2773, 2901, 2988, 3342, 3676.

2-Amino-4-oxo-4,7-dihydro-3*H*-pyrrolo[2,3-*d*]pyrimidine-5-carbaldehyde *O*-methyl oxime·HCl (25). To a suspension of *N*-((4-oxo-2-(tritylamino)-4,7-dihydro-3*H*-pyrrolo[2,3-d]-pyrimidin-5-yl)methyl)formamide (300 mg, 0.71 mmol) and Na_2SO_4 (5 mg) in MeOH (6 mL) was added methoxylamine hydrochloride (94.0 mg, 0.78 mmol) and triethylamine (156 μL, 0.78 mmol), the reaction mixture stirred at room temperature for 2 h. The volatiles were removed at reduced pressure and the residue dissolved in ethyl acetate before washing with 10% aqueous sodium bicarbonate solution. The organic phase was washed with brine, dried ($MgSO_4$) and concentrated *in vacuo* to yield the crude product which was purified by flash chromatography (7 : 3 hexane ethyl acetate) to yield the desired compound as a white solid (137 mg, 0.30 mmol, 43%), m.p. 186–190 °C.

A cooled (0 °C) solution of the trityl-protected compound (58 mg, 0.13 mmol) in 1 M HCl in dioxane (4.0 mL) was prepared and stirred for 10 minutes before the ice bath was removed and the reaction mixture stirred for 2 h at room temperature. The precipitated product was removed by filtration and washed with diethyl ether to yield the title compound as a white powder, (10 mg, 0.041 mmol, 32%), m.p. >250 °C (decomp.). ^{1}H NMR (400 MHz, DMSO-d_6): δ 3.87 (1H, s), 6.18 (2H, bs), 7.38 (1H, s), 7.84 (1H, s), 10.46 (1H, bs), 11.47 (1H, bs). ^{13}C NMR (100 MHz, DMSO-d_6): δ 61.7, 97.4, 108.7, 123.4, 138.8, 148.5, 152.6, 158.7. HRMS (m/z – ESI): found: 230.0668 ([M + Na]$^+$ $C_8H_9N_5NaO_2$; requires: 230.0654). ν_{max} (film)/cm^{-1}: 1053, 1593, 1672, 2854, 3132.

2-Amino-4-oxo-4,7-dihydro-3*H*-pyrrolo[2,3-*d*]pyrimidine-5-carbaldehyde oxime·HCl (26). To a suspension of *N*-((4-oxo-2-(tritylamino)-4,7-dihydro-3*H*-pyrrolo[2,3-*d*]pyrimidin-5-yl)-methyl)formamide (300 mg, 0.71 mmol) and Na_2SO_4 (5 mg) in MeOH (6 mL) was added *O*-(*tert*-butyldimethylsilyl)-hydroxylamine (120 mg, 0.81 mmol) the reaction mixture was stirred at room temperature for 2 h. The volatiles were removed at reduced pressure and the residue dissolved in ethyl acetate before washing with 10% aqueous sodium bicarbonate solution. The organic phase was washed with brine, dried ($MgSO_4$) and concentrated *in vacuo* to yield the crude product which was purified by flash chromatography (7 : 3 hexane ethyl acetate) to yield the desired compound as a white solid (220 mg, 0.40 mmol, 56%), m.p. >300 °C.

A cooled (0 °C) solution of the trityl-protected compound (203 mg, 0.37 mmol) in 1 M HCl in dioxane (4.0 mL) and methanol (1.0 mL) was prepared and stirred for 10 minutes at 0 °C before the ice bath was removed and the reaction mixture stirred for 2 h at room temperature. The precipitated product was removed by filtration and washed with diethyl ether to yield the title compound as an off-white powder, (70 mg, 0.30 mmol, 81%), m.p. >250 °C (decomp.). ^{1}H NMR (400 MHz, DMSO-d_6): δ 7.52 (1H, d, J 2.4), 7.84 (1H, s), 10.87 (1H, bs), 11.60 (1H, bs). ^{13}C NMR (100 MHz, DMSO-d_6): δ 97.9, 109.8, 124.0, 138.5, 144.3, 152.5, 158.4. HRMS (m/z – APCI): found: 192.0525 ([M − H]$^-$ $C_7H_6N_5O_2$; requires: 192.0521). ν_{max} (film)/cm^{-1}: 1578, 1671, 2625, 2971, 3088, 3676.

Conclusions

In summary, it has been found that a simple *in vitro* screen involving the measurement of IL-6 production by synovial fibroblasts from human RA patients could be used to select compounds for *in vivo* evaluation in murine EAE. The *in vitro*

assay revealed several deazaguanine QTRT substrates – from a library targeting side-chain rigidification – as being capable of reducing the levels of the key pro-inflammatory cytokine beyond that (relative to DMSO vehicle control) associated with the use of lead compound NPPDAG (**6**). In cases where the introduction of chain-rigidifying functionality also brought about (previously determined[25]) poorer QTRT substrate competency (*e.g.* **18** and **20**); commensurately weaker suppression of IL-6 production resulted. The somewhat unexpected superiority of the oxy-derivative of **6** (*i.e.* **23**) prompted the evaluation of simple oxime derivatives, which resulted in the identification of the considerably more potent derivatives **25** and **26**. Five deazaguanines were selected for full evaluation in murine EAE at concentrations equivalent to 15 mg Kg^{-1} of NPPDAG, all of which resulted in superior outcomes in terms of early arrest of disease progression and lower final clinical scores than when **6** was utilised. The *gem*-dimethyl analogue of **6** (*i.e.* **17**) and the methyl oxime **25** appear particularly promising and warrant further investigation. The emergence of the oximes as active candidates is fascinating given that they are excellent QTRT substrates yet are located outside the chemical space outlined in extensive previous SAR studies focused on molecules related to **6**. In this regard it is interesting that the genotoxic QTRT substrate 6-thioguanine (which also represents a considerably truncated pharmacophore relative to **6**) has also been shown to be active against EAE in mice without the HPRT enzyme (responsible for its toxicity).[28] At this juncture, it appears that a small *O*-substituent in the oxime series (*i.e.* –H or Me) and an O-atom replacing the C-atom adjacent to the methylene amine in derivatives of **NPPDAG** are most beneficial from an activity standpoint. Investigations to determine (*inter alia*) if the oximes operate in a similar fashion to 6-thioguanine without the attendant genotoxicity are underway.

Author contributions

S. J. C., J. M. S., V. P. K. and U. F. designed the experimental protocol and drafted the manuscript. M. C. performed the synthesis of the candidate molecules. S. M. Q. performed the EAE experiments and S. A. and T. R. performed the *in vitro* assays. All authors read and approved the final manuscript.

Conflicts of interest

S. J. C., J. M. S. and V. P. K. are founders of a company – Azadyne Ltd. – involved in developing drug candidates for the treatment of autoimmune disease. No data or savoir-faire generated by Azadyne is incorporated into this manuscript.

Acknowledgements

Financial support from the School of Chemistry, Trinity College Dublin for a studentship for M. C. is gratefully acknowledged. The work described herein also emanated from research conducted with the financial support of Science Foundation Ireland under Grant number 17/TIDA/5029 and Enterprise Ireland Grant number CF/2015//0029. For the purpose of Open Access, the author has applied a CC BY public copyright licence to any Author Accepted Manuscript version arising from this submission.

References

1 D. S. Reich, C. F. Lucchinetti and P. A. Calabresi, *N. Engl. J. Med.*, 2018, **378**, 169–180.
2 C. Walton, R. King, L. Rechtman, W. Kaye, E. Leray, R. A. Marrie, N. Robertson, N. La Rocca, B. Uitdehaag, I. van der Mei, M. Wallin, A. Helme, C. A. Napier, N. Rijke and P. Baneke, *Mult. Scler.*, 2020, **26**, 1816–1821.
3 J. H. Yang, T. Rempe, N. Whitmire, A. Dunn-Pirio and J. S. Graves, *Front. Neurol.*, 2022, **13**, 824926.
4 L. Bierhansl, H.-P. Hartung, O. Aktas, T. Ruck, M. Roden and S. G. Meuth, *Nat. Rev. Drug Discovery*, 2022, **21**, 578.
5 C. Fergus, D. Barnes, M. A. Alqasem and V. P. Kelly, *Nutrients*, 2015, **7**, 2897–2929.
6 N. Okada, F. Harada and S. Nishimura, *Nucleic Acids Res.*, 1976, **3**, 2593–2603.
7 N. Shindo-Okada, N. Okada, T. Ohgi, T. Goto and S. Nishimura, *Biochemistry*, 1980, **19**, 395–400.
8 Y.-C. Chen, V. P. Kelly, S. V. Stachura and G. A. Garcia, *RNA*, 2010, **16**, 958–968.
9 M. A. Alqasem, C. Fergus, J. M. Southern, S. J. Connon and V. P. Kelly, *Chem. Commun.*, 2020, **56**, 3915–3918.
10 M. Sebastiani, C. Behrens, S. Dörr, H.-D. Gerber, R. Benazza, O. Hernandez-Alba, S. Cianférani, G. Klebe, A. Heine and K. Reuter, *ACS Chem. Biol.*, 2022, **17**, 2229–2247.
11 W. R. Farkas, *J. Biol. Chem.*, 1980, **255**, 6832–6835.
12 J. R. Katze, B. Basile and J. A. McCloskey, *Science*, 1982, **216**, 55–56.
13 T. Rakovich, C. Boland, I. Bernstein, V. M. Chikwana, D. Iwata-Reuyl and V. P. Kelly, *J. Biol. Chem.*, 2011, **286**, 19354–19363.
14 T. Tuorto, C. Legrand, C. Cirzi, G. Federico, R. Liebers, M. Müller, A. E. Ehrenhofer-Murray, G. Dittmar, H.-J. Gröne and F. Lyko, *EMBO J.*, 2018, **37**, e99777.
15 M. Müller, C. Legrand, F. Tuorto, V. P. Kelly, Y. Atlasi, F. Lyko and A. E. Ehrenhofer-Murray, *Nucleic Acids Res.*, 2019, **47**, 3711–3727.
16 P. Hayes, C. Fergus, M. Ghanim, C. Cirzi, L. Burtnyak, C. J. McGrenaghan, F. Tuorto, D. P. Nolan and V. P. Kelly, *Nutrients*, 2020, **12**, 871.
17 Y. L. Chen and R. T. Wu, *Cancer Res.*, 1994, **54**, 2192–2198.
18 C. J. Morgan, F. L. Merrill and R. W. Trewyn, *Cancer Res.*, 1996, **56**, 594–598.
19 P. Thumbs, T. T. Ensfelder, M. Hillmeier, M. Wagner, M. Heiss, C. Scheel, A. Schön, M. Müller, S. Michalakis, S. Kellner and T. Carell, *Angew. Chem., Int. Ed.*, 2020, **59**, 12352–12356.
20 B. S. Huang, R. T. Wu and K. Y. Chien, *Cancer Res.*, 1992, **52**, 4696–4700.
21 W. Baranowski, G. Dirheimer, J. A. Jakowicki and G. Keith, *Cancer Res.*, 1994, **54**, 4468–4471.

22 G. Dirheimer, W. Baranowski and G. Keith, *Biochimie*, 1995, **77**, 99–103.
23 P. J. Eggenhuizen, B. H. Ng and J. D. Ooi, *Int. J. Mol. Sci.*, 2020, **21**, 7015.
24 T. K. Goswami, M. Singh, M. Dhawan, S. Mitra, T. Bin Emran, A. A. Rabaan, A. Al Mutair, Z. Al Alawi, S. Alhumaid and K. Dhama, *Hum. Vaccines Immunother.*, 2022, **18**, 2035117.
25 C. Fergus, M. Al-qasem, M. Cotter, C. M. McDonnell, E. Sorrentino, F. Chevot, K. Hokamp, M. O. Senge, J. M. Southern, S. J. Connon and V. P. Kelly, *Nucleic Acids Res.*, 2021, **49**, 4877–4890.
26 W. R. Farkas, K. B. Jacobson and J. R. Katze, *Biochim. Biophys. Acta*, 1984, **781**, 64–75.
27 R. P. Singhal, R. A. Kopper, S. Nishimura and N. Shindo-Okada, *Biochem. Biophys. Res. Commun.*, 1981, **99**, 120–126.
28 S. Varghese, M. Cotter, F. Chevot, C. Fergus, C. Cunningham, K. H. Mills, S. J. Connon, J. M. Southern and V. P. Kelly, *Nucleic Acids Res.*, 2017, **45**, 2029–2039.
29 M. Cotter, S. Varghese, F. Chevot, C. Fergus, V. P. Kelly, S. J. Connon and J. M. Southern, *ChemMedChem*, 2023, **18**, e202300207.
30 S. Shams, J. M. Martinez, J. R. D. Dawson, J. Flores, M. Gabriel, G. Garcia, A. Guevara, K. Murray, N. Pacifici, M. V. Vargas, T. Voelker, J. W. Hell and J. F. Ashouri, *Front. Pharmacol.*, 2021, **12**, 680043.
31 P. Luo, P. Wang, J. Xu, W. Hou, P. Xu and K. Xu, *Bone Joint Res.*, 2022, **11**, 426–438.
32 F. Pandolfi, L. Franza, V. Carusi, S. Altamura, G. Andriollo and E. Nucera, *Int. J. Mol. Sci.*, 2020, **21**, 5238.
33 P. Zafari, M. Taghadosi, F. Faramarzi, M. Rajabinejad and A. Rafiei, *Inflammation*, 2023, **46**, 612–622.
34 G. Montes Diaz, R. Hupperts, J. Fraussen and V. Somers, *Autoimmun. Rev.*, 2018, **17**, 1240–1250.
35 I. M. Stromnes and J. M. Goverman, *Nat. Protoc.*, 2006, **1**, 1810–1819.